



Shiraz University  
Faculty of Engineering

**Ph.D. Thesis**  
**In**  
**Materials Science and Engineering**

**Investigation of ZnO-based nanostructured dye-sensitized  
solar cell electrodes**

**By:**  
Ahmad Irannejad Parizi

**Supervised by:**  
Prof. K. Janghorban

January 2012

*In the name of God*

IN THE NAME OF GOD

INVESTIGATION OF ZnO-BASED NANOSTRUCTURED  
DYE-SENSITIZED SOLAR CELL ELECTRODES

BY

AHMAD IRANNEJAD PARIZI





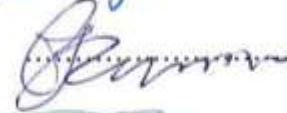

THESIS

SUBMITTED TO THE SCHOOL OF GRADUATE STUDIES IN PARTIAL FULFILLMENT  
OF THE REQUIREMENTS FOR THE DEGREE OF DOCTOR OF PHILOSOPHY (PH.D.)

IN

MATERIALS SCIENCE AND ENGINEERING  
SHIRAZ UNIVERSITY  
SHIRAZ  
ISLAMIC REPUBLIC OF IRAN

EVALUATED AND APPROVED BY THE THESIS COMMITTEE AS: EXCELLENT

 K. JANGHORBAN, PH.D., PROF. OF MATERIALS  
SCIENCE AND ENGINEERING (CHAIRMAN)  
 M.E. BAHROLOLOOM, PH.D., PROF. OF MATERIALS  
SCIENCE AND ENGINEERING  
 B. HASHEMI, PH.D., ASSISTANT PROF. OF  
MATERIALS SCIENCE AND ENGINEERING  
 A. DEGHAN, PH.D., ASSISTANT PROF. OF  
MATERIALS SCIENCE AND ENGINEERING  
 G. KARIMI, PH.D., ASSOCIATE PROF. OF  
CHEMICAL ENGINEERING  
 N. TAGHAVINIA, PH.D., ASSOCIATE PROF. OF  
PHYSICS

JANUARY 2012

## **Acknowledgements**

I wish to express my sincere appreciation to my supervisor, Prof. Kamal Janghorban, for his continuous guidance, support, and encouragement throughout this research and for my future academic career. He gave me a high degree of freedom and always encouraged me to explore novel research directions which I'm interested in. This has been the most valuable experience I have had during my whole graduate study at Shiraz University. I would like to thank my committee members, Dr. Bahrololoom, Dr. Hashemi, Dr. Dehghan, Dr. Taghavinia, and Dr. Karimi for their support and correction of my thesis.

I would also like to thank my sabbatical supervisor, Prof. Tan Ooi Kiang, for his support, and encouragement during my stay at Nanyang Technological University (NTU), Singapore. I am grateful to the members of his research group, who helped and supported me during my study there, including Dr. Huang Hui, Tan Pei Yun, Fang Xiaoqin, Lim Chiew Keat, and Chua Chin Sheng. I also like to thank all the staffs of the Sensor and Actuator Lab of the School of Electrical and Electronic Engineering at NTU, Singapore.

I would also like to thank my friends, Saeed Maleksaeedi, Mohammad Ghaffari, and Mohammad Shahjamali, for their helps.

Lastly, I would like to thank my wife, my parents, and my whole family for their endless love, sacrifice, support, understanding and encouragement. Without them, I could not have made it.

# **ABSTRACT**

## **INVESTIGATION OF ZnO-BASED NANOSTRUCTURED DYE-SENSITIZED SOLAR CELL ELECTRODES**

BY

AHMAD IRANNEJAD PARIZI

With increasing consumption of energy, non-fossil energy sources such as solar energy are being considered intensely. In this study several different morphologies of nanostructured ZnO arrays were produced as photo-anode electrodes of dye-sensitized solar cells. Fluorine-doped tin oxide (FTO) substrate was pre-modified with a ZnO thin film as a seed layer by Sol-Gel coating. Then, well-aligned ZnO nanorod arrays with high aspect ratio have been grown on the substrate by hydrothermal process. TiO<sub>2</sub> thin shells with different thickness were grown on the ZnO nanorods by chemical vapor deposition (CVD) method, which improved the cell efficiency. Also flower like ZnO nanosheets, and globular ZnO, which it was a novel structure, were grown on FTO substrates by chemical bath deposition (CBD). Dendritic structures were produced by growing the ZnO nanorods on flower like ZnO nanosheets which it was different from others. Sample characterization was performed by X-ray diffraction (XRD), electron microscopy (SEM, FESEM, TEM, and SAD), X-ray photoelectron spectroscopy (XPS), and UV-vis Spectroscopy. The nanorod diameter distribution was obtained from SEM and FESEM images. The diameter of the ZnO nanorods ranged from about 30nm to more than 100nm and their lengths were about 6 $\mu$ m for 12 hours hydrothermal process. XRD and TEM analysis indicated a wurtzite structure with high crystallinity and confirmed that each individual ZnO nanorod was a single crystal. XPS and TEM results confirmed the formation of a TiO<sub>2</sub> film on the ZnO nanorods. UV-vis Spectroscopy showed that the transmittance of ZnO nanosheets layers was more than ZnO nanorods sample with the same thickness in the visible range. The photoelectrochemical experiments were performed in a sandwich type

two-electrode cell and  $J$ - $V$  curves were obtained. Results of the test of ZnO nanorods based solar cells, showed that by increasing the thickness of ZnO nanorods layer, efficiency improved slightly and then decreased for higher thickness values. The results of solar cell testing showed that coating of TiO<sub>2</sub> shells on ZnO nanorod significantly increased the short circuit current ( $J_{SC}$ ), open circuit voltage ( $V_{OC}$ ), fill factor and efficiency relative to devices without TiO<sub>2</sub> shells. Overall cell efficiency jumped from 0.45% for bare ZnO nanorode array to 0.92% for 14 nm thick TiO<sub>2</sub> shells on ZnO which showed a two fold increase. The fill factor increased from 0.37 to 0.60, showing a 62% improvement. For a TiO<sub>2</sub> shell 21 nm thick,  $V_{OC}$  increased from 0.53V, to 0.68 V. The results showed that it is possible to fabricate core-shell cells of higher efficiency by using nanorod arrays. Using ZnO nanosheets and globular ZnO electrodes instead of ZnO nanorods, improved the  $J_{SC}$ ,  $V_{OC}$ , fill factor and solar cell efficiency. Using ZnO nanosheets electrodes instead of ZnO nanorods, increased the cell efficiency from 0.45% to 2.9%, which showed a several fold increase. Overall conversion efficiency about 3.8% was obtained for globular ZnO electrodes. Also by using dendritic structures of ZnO the cell efficiency and other parameters were improved, which was due to the high surface area. Increased thickness of ZnO nanosheets and globular structures layers improved the efficiency several times, which was not possible for ZnO nanorod. Design of experiments via Taguchi methods was done and the optimum condition was obtained. The results of solar cell tests showed that sensitization time was an important parameter in the ZnO based dye-sensitized solar cell efficiency and the highest efficiency was obtained for 30 minutes sensitization time.

## Table of contents

<b>Subject .....</b>	<b>page</b>
List of figures .....	XI
List of tables .....	XX
Chapter one: Introduction .....	2
Chapter two: Literature review .....	5
2.1. Introduction.....	5
2.2. The principles of photovoltaic .....	5
2.3. Physical basis of the solar cell .....	6
2.4. History of photovoltaic .....	8
2.5. Development of solar cell .....	10
2.6. Dye-sensitized solar cells.....	11
2.6.1. History of the development of DSSCs .....	12
2.6.2. Operational principle of the DSSCs .....	12
2.7. General properties of ZnO .....	15
2.7.1. Background for ZnO.....	15
2.7.2. Crystal structures of ZnO.....	15
2.7.3. Physical properties of ZnO .....	17
2.8. Sol-Gel synthesis of ZnO thin film.....	18
2.9. Hydrothermal method of ZnO nanorod synthesis .....	19
2.10. Chemical bath deposition of ZnO nanostructures .....	21
2.11. Zinc oxide based DSSCs.....	23
2.12. Nanostructure ZnO for DSSCs .....	26
2.12.1. ZnO nanoparticulate film.....	27
2.12.2. Nanoporous structure ZnO film.....	29

<b>Subject .....</b>	<b>page</b>
2.12.3. Nanostructures with direct pathways for electron transport .....	32
2.12.3.1. ZnO Nanowires.....	32
2.12.3.2. ZnO Nanotubes .....	34
2.12.3.3. ZnO Nanoflowers .....	35
2.12.3.4. Dendritic ZnO Nanowires .....	36
2.12.4. Other nanostructure ZnO films.....	38
2.12.4.1. Nanosheets .....	38
2.12.4.2. Nanobelts .....	39
2.12.4.3. Tetrapods .....	39
2.13.Design of experiments via Taguchi methods.....	41
2.13.1. Introduction to Taguchi methods.....	41
2.13.2. Summary of Taguchi method .....	43
2.13.3. Taguchi loss function.....	44
2.13.4. Determining parameter design orthogonal array .....	45
2.13.5. Analyzing experimental data .....	48
2.13.6. Advantages and disadvantages of Taguchi method ...	51
2.13.7. Using Taguchi method in current study .....	52
Chapter three: Experimental procedure .....	54
3.1. Materials synthesis.....	54
3.1.1. Primary materials.....	54
3.1.2. Sol-Gel synthesis of ZnO thin film.....	54
3.1.3. Growth of ZnO nanorods array .....	55
3.1.4. Deposition of TiO <sub>2</sub> shells on ZnO nanorods .....	56
3.1.4.1.Sol-Gel synthesis of TiO <sub>2</sub> shell .....	56
3.1.4.2.Chemical vapor deposition of TiO <sub>2</sub> shell .....	57
3.1.5. Growth of flower like ZnO nanosheets .....	58
3.1.6. Globular ZnO grown by chemical bath deposition .....	59
3.1.7. Dendritic structure obtained by growing ZnO nanorods on the ZnO nanosheets .....	59
3.2. Materials characterization.....	60



<b>Subject .....</b>	<b>page</b>
3.2.1. Thermal analysis tests.....	60
3.2.2. Electrical and optical properties measurement.....	61
3.2.3. Microstructure studies .....	63
3.2.4. Solar cell fabrication.....	63
3.2.4.1.Preparation of nanostructured ZnO photo-anode electrodes .....	63
3.2.4.2.Fabrication of TiO <sub>2</sub> light-scattering layer.....	63
3.2.4.3.Thickness measurement.....	64
3.2.4.4.Synthesis of ruthenium sensitizer .....	65
3.2.4.5.Immersing the nanostructured photo-anode electrode into the dye solution .....	65
3.2.4.6.Preparation of counter Pt-electrodes .....	66
3.2.4.7.Preparation of electrolyte.....	66
3.2.4.8.DSSC assemblage.....	66
3.2.4.9.Photovoltaic measurements .....	66
3.3. Optimization of experimental parameters based on the Taguchi robust design .....	68
Chapter four: Results and discussion .....	70
4.1. Sol-Gel synthesis of ZnO thin film.....	70
4.1.1. Hall effect measurement .....	70
4.1.2. TGA-DTA tests .....	71
4.1.3. Scanning electron microscopy .....	71
4.1.4. UV-vis spectrometer measurement .....	73
4.2. Growth of ZnO nanorods array.....	75
4.2.1. Scanning electron microscopy .....	75
4.2.2. Field emission scanning electron microscopy .....	80
4.2.3. Transmission electron microscopy .....	85
4.2.4. UV-vis spectrometer measurement .....	86
4.2.5. X-ray diffraction analysis .....	87
4.2.6. X-ray photoelectron spectroscopy (XPS) .....	88
4.2.7. Solar cell fabrication and testing .....	89

<b>Subject .....</b>	<b>page</b>
4.2.7.1. Effect of ZnO nanorods film thickness on the solar cell efficiency .....	89
4.3. Deposition of TiO <sub>2</sub> shells on ZnO nanorods.....	91
4.3.1. Transmission electron microscopy .....	91
4.3.2. X-ray photoelectron spectroscopy (XPS) .....	92
4.3.3. Solar cell fabrication and testing .....	95
4.3.3.1. Effect of TiO <sub>2</sub> shells grown by Sol-Gel synthesis on the cell efficiency .....	95
4.3.3.2. Effect of TiO <sub>2</sub> shells grown by chemical vapor deposition on the cell efficiency .....	98
4.4. Growth of flower like ZnO nanosheets .....	102
4.4.1. TGA-DTA tests .....	102
4.4.2. Scanning electron microscopy .....	103
4.4.3. Field emission scanning electron microscopy .....	105
4.4.4. X-ray diffraction analysis .....	108
4.4.5. X-ray photoelectron spectroscopy (XPS) .....	109
4.4.6. Solar cell fabrication and testing .....	109
4.4.7. UV-vis spectrometer measurement .....	111
4.5. Globular ZnO grown by chemical bath deposition .....	112
4.5.1. Field emission scanning electron microscopy .....	112
4.5.2. X-ray diffraction analysis .....	115
4.5.3. Solar cell fabrication and testing .....	115
4.6. Dendritic structure obtained by growing ZnO nanorods on the ZnO nanosheets .....	117
4.6.1. Scanning electron microscopy .....	117
4.6.2. Solar cell fabrication and testing .....	120
4.7. Design of experiments via Taguchi methods.....	124
4.7.1. Selection of factors and their levels.....	125
4.7.2. Analyzing experimental data .....	126
4.7.3. Prediction and confirmation of properties .....	128
Chapter five: Conclusions and future works.....	131

<b>Subject .....</b>	<b>page</b>
5.1. Conclusions.....	131
5.2. Future works .....	133
References .....	134

## List of figures

<b>Subject .....</b>	<b>page</b>
Fig. 2-1. A schematic of a simple conventional solar cell. Creation of electron-hole pairs, $e^-$ and $h^+$ , respectively, is depicted. ....	7
Fig. 2-2. Schematic of a typical $TiO_2$ nanoparticle-based DSSC. Dye molecules attach the surface of the nanoparticle film and the electrolyte penetrates between the semiconductor pores forming a semiconductor-dye-electrolyte interface of high surface area. ....	13
Fig. 2-3. Energy band diagram of a $TiO_2$ nanoparticle-based DSSC. A dye molecule absorbs a photon and promotes an electron to an excited state. The excited electron is injected into the $TiO_2$ nanoparticle and diffuses to the TCO anode. The hole left on the dye is transferred to the electrolyte and diffuses to the cathode where it recombines with an electron. The maximum DSSC photovoltage is given by the difference between the conduction band energy level of the semiconductor and the redox potential level of the electrolyte ..	14
Fig. 2-4. Stick and ball models of three crystalline structures of ZnO. Atoms with the same color of the corner ones are O atoms and those of the other kind are Zn atoms. ....	16
Fig. 2-5. A unit cell of wurtzite ZnO. ....	17
Fig. 2-6. A chemical bath for the deposition of layered hydroxide ....	22
Fig. 2-7. A collection of nanostructures of ZnO synthesized under ...	26
Fig. 2-8. SEM image of a ZnO-nanoparticle electrode prepared with a compression method .....	29

**Subject ..... page**

Fig. 2-9. Schematic diagram of the nanowire-based DSSC.  
 Nanowires may provide electrons with a direct path and may improve the collection efficiency..... 32

Fig. 2-10. Cross-sectional SEM image of the ZnO-nanowire array. ... 34

Fig. 2-11. SEM images of a ZnO-nanoflower film..... 35

Fig. 2-12. Cross-sectional SEM images of dendritic ZnO nanowires after two generations of growth..... 37

Fig. 2-13. SEM images of nanostructured ZnO films: a) Dispersed nanosheets, b) Nanosheet-assembled spheres, c) Nanobelt array, d) Networked film with interconnected ZnO tetrapods.... 39

Fig. 3-1. Atmospheric pressure chemical vapor deposition (APCVD) system which was used for TiO<sub>2</sub> shell coating. .... 58

Fig. 3-2. TGA-DTA measurement system (DTG-60H). .... 60

Fig. 3-3. Software view of TGA-DTA measurement system. .... 60

Fig. 3-4. Hall Effect measurement system (HL5500)..... 61

Fig. 3-5. Software view of Hall Effect measurement system. .... 61

Fig. 3-6. UV-vis Spectrometer (Shimadzu UV-2450)..... 62

Fig. 3-7. Software view UV-vis Spectrometer system. .... 62

Fig. 3-8. Surface profiler system (DEKTAK3). .... 64

Fig. 3-9. Software view of surface profiler system..... 64

Fig. 3-10. Dye-sensitized electrode which was prepared for solar cell fabrication..... 65

Fig. 3-11. Configuration of the dye sensitized solar cells ..... 67

Fig. 3-12. Solar simulator system, (a) before, and (b) during the solar cell testing. .... 67

Fig. 3-13. Software view of the photovoltaic measurement system... 68

Fig. 4-1. TGA-DTA diagram of dried gel of ZnO Sol-Gel coating. .. 71

Fig. 4-2. Uniform ZnO thin film on FTO substrate produced by Sol-Gel coating. (ZnO Sol-Gel solution concentration: 0.05M). (a) Typical SEM image, (b) EDX analysis spectrum, (c) and (d) EDX map of Zinc and Oxygen. .... 72

**Subject ..... page**

Fig. 4-3. FESEM image of ZnO thin film on FTO substrate at different magnification, produced by Sol-Gel coating (solution concentration: 0.05M). ..... 73

Fig. 4-4. UV-visible transmittance spectrum of the FTO glass. .... 74

Fig. 4-5. UV-visible absorption spectrum of the FTO glass and ZnO thin film coated FTO glass (ZnO Sol-Gel solution concentration: 0.05M). ..... 74

Fig. 4-6. SEM image of non-uniform ZnO nanorod, because of technical problem of hydrothermal process. The concentrations of both  $Zn(NO_3)_2$  and methenamine in hydrothermal solution are 0.05M. Growth time: 4 h. .... 75

Fig. 4-7. SEM image of non-uniform ZnO nanorod, because of non-uniform seed layer. The concentrations of both  $Zn(NO_3)_2$  and methenamine in hydrothermal solution are 0.05M. Growth time: 4 h. .... 76

Fig. 4-8. SEM image of non-uniform ZnO nanorod which growth on different kind of seed layer. The concentrations of zinc acetate for Sol-Gel solution are (a) 0.005 M, (b) 0.010 M, (c) 0.020M and (d) 0.040M. The concentrations of both  $Zn(NO_3)_2$  and methenamine in hydrothermal solution are 0.025M for all samples. Growth time: 4 h. .... 77

Fig. 4-9. SEM image of well-aligned ZnO nanorod arrays grown on FTO substrate at 95°C. The concentrations of both  $Zn(NO_3)_2$  and methenamine in mixed solution are 0.025M. Growth time: 4 h. (a), (b), (c), and (d) top view. (e) and (f) 45° tilt view. (g) and (h) side view. .... 78

Fig. 4-10. SEM image of well-aligned ZnO nanorod arrays grown on FTO substrate at 95°C. The concentrations of both  $Zn(NO_3)_2$  and methenamine in mixed solution are 0.05M. Growth time: 4 h. (a), (b), (c), and (d) top view. (e) and (f) 45° tilt view. (g) and (h) side view. .... 79

**Subject ..... page**

Fig. 4-11. SEM image ZnO nanorod arrays grown on FTO substrate at 95°C, (top view). The concentrations of both Zn(NO<sub>3</sub>)<sub>2</sub> and methenamine in mixed solution are 0.075M. Growth time: 4 h. .... 80

Fig. 4-12. FESEM image of non-uniform ZnO nanorod because of non-continues seed layer due to dilute Sol-Gel solution. ZnO Sol-Gel solution concentration for the seed layer: 0.005M. The concentrations of both Zn(NO<sub>3</sub>)<sub>2</sub> and methenamine in hydrothermal solution are 0.025M. Hydrothermal growth time: 4 h. .... 81

Fig. 4-13. FESEM image of non-uniform ZnO nanorod because of non-uniform seed layer. The concentrations of both Zn(NO<sub>3</sub>)<sub>2</sub> and methenamine in hydrothermal solution are 0.025M. Hydrothermal growth time: 4 h..... 82

Fig. 4-14. FESEM image of uniform ZnO nanorod on FTO substrate at 95°C. The concentrations of both Zn(NO<sub>3</sub>)<sub>2</sub> and methenamine in mixed solution are 0.01M. Growth time: 4 h... 83

Fig. 4-15. FESEM image of uniform ZnO nanorod on FTO substrate at 95°C. The concentrations of both Zn(NO<sub>3</sub>)<sub>2</sub> and methenamine in mixed solution are 0.025M. Growth time: 4h.. 83

Fig. 4-16. FESEM image of uniform ZnO nanorod on FTO substrate at 95°C. The concentrations of both Zn(NO<sub>3</sub>)<sub>2</sub> and methenamine in mixed solution are 0.05M. Growth time: 4 h... 83

Fig. 4-17. FESEM image of uniform ZnO nanorod on FTO substrate at 95°C with different concentrations of Zn(NO<sub>3</sub>)<sub>2</sub> and methenamine in mixed solution (a) 0.01M, (b) 0.025M, and (c) 0.05M. Growth time: 4 h. .... 84

Fig. 4-18. EM image of ZnO nanorods at different magnification..... 85

Fig. 4-19. TEM images of ZnO nanorod (a) (b) low-magnification image, (c) High-resolution TEM image, (d) corresponding selected area electron diffraction pattern (SAED)..... 86

<b>Subject .....</b>	<b>page</b>
Fig. 4-20. Typical UV–vis spectrum of as-grown ZnO nanorods. ....	87
Fig. 4-21. XRD pattern of ZnO nanorod arrays on FTO substrate (*), (a) 0.005 M, (b) 0.010 M, (c) 0.025M, (d) 0.050M, and Standard ZnO (JCPDS No.36-1451). (concentrations are for both Zn(NO <sub>3</sub> ) <sub>2</sub> and methenamine in hydrothermal solution). Growth time: 4 h. ....	88
Fig. 4-22. XPS Survey scan spectrum of ZnO nanorods with different dye sensitization time. (a) without sensitization, (b) 1h, (c) 12h, and (d) 18h.....	89
Fig. 4-23. Current-voltage characteristics of the DSSCs constructed using the different thickness of ZnO nanorod arrays. ....	90
Fig. 4-24. TEM images of ZnO-TiO <sub>2</sub> Core-Shell structure, (a) and (b) low-magnification image, (c) high-magnification image, and (d) corresponding selected area electron diffraction pattern (SAED). ....	91
Fig. 4-25. TEM images of ZnO-TiO <sub>2</sub> Core-Shell structure with TiO <sub>2</sub> nano particles.....	92
Fig. 4-26. Wide scan survey XPS spectrum of (a) ZnO nanorod, (b) TiO <sub>2</sub> coated ZnO nanorod. ....	93
Fig. 4-27. (a) XPS spectrum in the O 1s region for ZnO nanorod and TiO <sub>2</sub> coated ZnO nanorod, and (b) narrow scan of Ti 2p. ...	94
Fig. 4-28. J-V curves of primary solar cells from ZnO nanorod electrode with and without TiO <sub>2</sub> Sol-Gel coating. (a) 0.050M, ZnO nanorods, (b) 0.025M, ZnO nanorods, (c) 0.050M, ZnO nanorods with TiO <sub>2</sub> Sol-Gel coating, and (d) 0.025M, ZnO nanorods with TiO <sub>2</sub> Sol-Gel coating, (concentrations are for both Zn(NO <sub>3</sub> ) <sub>2</sub> and methenamine in hydrothermal solution, spin coater rotation speed: 2500 rpm, TiO <sub>2</sub> Sol-Gel solution concentration: 0.1M )......	95



**Subject ..... page**

Fig. 4-29. Current-voltage characteristics of the DSSCs constructed using the ZnO nanorod arrays and ZnO nanorods with TiO<sub>2</sub> Shell produced by Sol-Gel coating (concentrations of hydrothermal solution: 0.05M, Sol-Gel solution concentration: 0.1M, spin coater rotation speed: 4500 rpm). .... 97

Fig. 4-30. Current-voltage characteristics of the DSSCs constructed using the ZnO nanorod arrays, and the TiO<sub>2</sub> coated ZnO nanorods with different shell thickness..... 98

Fig. 4-31. (a)Dependence of  $V_{OC}$  and fill factor on the thickness of the TiO<sub>2</sub> shell, and (b) Dependence of  $J_{SC}$  and cell efficiency on the thickness of the TiO<sub>2</sub> shell for ZnO-TiO<sub>2</sub> core-shell nanorod cells. .... 100

Fig. 4-32. Dependence of cell efficiency on the thickness of the TiO<sub>2</sub> shell. .... 102

Fig. 4-33. TGA-DTA diagram of flower like ZnO nanosheets. .... 103

Fig. 4-34. SEM photos of flower like nanosheets at different magnification, before sintering process. Zinc acetate concentration: 0.15 M, solution temperature: 60 °C, deposition process time: 40 h. (a), (b), (c), and (d) Top view. (e), (f), (g), and (h) Side view. .... 104

Fig. 4-35. SEM photos of flower like ZnO nanosheets at different magnification, after sintering process. Zinc acetate concentration: 0.15 M, solution temperature: 60 °C, deposition time: 40 h, sintering temperature: 450 °C, sintering time: 1 h. (a), (b), (c), and (d) Top view. (e) and (f) Side view..... 105

Fig. 4-36. FESEM Photos of flower like ZnO nanosheets, after heating at different magnification, (Zinc acetate concentration: 0.15 M, solution temperature: 60 °C, deposition process time: 40 h, sintering temperature: 450 °C, sintering time: 1 h). .... 106

<b>Subject .....</b>	<b>page</b>
Fig. 4-37. FESEM Photos of flower like ZnO nanosheets, after heating at different magnification, (Zinc acetate concentration: 0.15 M, solution temperature: 60 °C, deposition process time: 48 h, sintering temperature: 450 °C, sintering time: 1 h).....	106
Fig. 4-38. FESEM Photos of flower like ZnO nanosheets, after heating at different magnification, (Zinc acetate concentration: 0.15 M, solution temperature: 60 °C, deposition process time: 52 h, sintering temperature: 450 °C, sintering time: 1 h).....	106
Fig. 4-39. FESEM Photos of flower like ZnO nanosheets, after heating for different deposition process time. Zinc acetate concentration: 0.15 M, solution temperature: 60 °C, and the deposition time of (a) 40 h, (b) 48 h, and (c) 52 h.....	107
Fig. 4-40. XRD pattern of typical ZnO nanosheets structure on FTO substrate (*). .....	108
Fig. 4-41. XPS spectrum of ZnO nanosheets (a) before, and (b) after heating.....	109
Fig. 4-42. Current-voltage characteristics of the DSSCs constructed using the ZnO nanorod arrays and the ZnO nanosheets with different thickness. ....	110
Fig. 4-43. Results of testing different kind of solar cells.....	111
Fig. 4-44. UV–vis spectrum of ZnO nanorods and ZnO nanosheets samples with the same thickness. ....	112
Fig. 4-45. FESEM Photos of globular ZnO grown by chemical bath deposition at different magnification. Zinc acetate concentration: 0.15 M, solution temperature: 60 °C, (Deposition time: 36 h). .....	113

**Subject ..... page**

Fig. 4-46. FESEM Photos of globular ZnO grown by chemical bath deposition at different magnification. Zinc acetate concentration: 0.15 M, solution temperature: 60 °C, (Deposition time: 40 h). ..... 113

Fig. 4-47. FESEM Photos of globular ZnO grown by chemical bath deposition at different magnification. Zinc acetate concentration: 0.15 M, solution temperature: 60 °C, (Deposition time: 48 h). ..... 113

Fig. 4-48. FESEM Photos of globular ZnO grown by chemical bath deposition, for different deposition process time. Zinc acetate concentration: 0.15 M, solution temperature: 60 °C, and the deposition time of (a) 36 h, (b) 40 h, and (c) 48 h. .... 114

Fig. 4-49. XRD pattern of globular ZnO structure on FTO substrate (\*). ..... 115

Fig. 4-50. Current-voltage characteristics of the DSSCs constructed using the globular ZnO structure with different deposition time. .... 116

Fig. 4-51. SEM Photos of ZnO dendritic nanostructure grown by chemical bath deposition and hydrothermal process (hydrothermal process time: 4h). (a), (b), (c), and (d) Top view. (e), (f), (g), and (h) Side view. .... 118

Fig. 4-52. SEM Photos of ZnO dendritic nanostructure grown by chemical bath deposition and hydrothermal process (hydrothermal process time: 12h). (a), (b), (c), and (d) Top view. (e), (f), (g), and (h) Side view. .... 119

Fig. 4-53. Current-voltage characteristics of the DSSCs constructed using the ZnO nanosheets and dendritic structure of ZnO. .... 120

Fig. 4-54. Schematic diagram of the possible electron transport mechanism in the DSSC photoanode consisting of the hierarchical ZnO nanowire-nanosheet architectures. .... 123

<b>Subject .....</b>	<b>page</b>
Fig. 4-55. Results of testing different kind of solar cells.....	124
Fig. 4-56. SN ratio graph for solar cells efficiency and standard deviation.....	128